applied sciences

MDPI

Article

WFT-Fati-Dec: Enhanced Fatigue Detection AI System Based on Wavelet Denoising and Fourier Transform

Ahmed Sedik [1,2,*], Mohamed Marey [1] and Hala Mostafa [3,*]

1 Smart Systems Engineering Laboratory, College of Engineering, Prince Sultan University, Riyadh 11586, Saudi Arabia
2 Department of the Robotics and Intelligent Machines, Faculty of Artificial Intelligence, Kafrelsheikh University, Kafrelsheikh 33516, Egypt
3 Department of Information Technology, College of Computer and Information Sciences, Princess Nourah Bint Abdulrahman University, P.O. Box 84428, Riyadh 11671, Saudi Arabia
* Correspondence: asedik@psu.edu.sa (A.S.); hfmostafa@pnu.edu.sa (H.M.)

Abstract: As the number of road accidents increases, it is critical to avoid making driving mistakes. Driver fatigue detection is a concern that has prompted researchers to develop numerous algorithms to address this issue. The challenge is to identify the sleepy drivers with accurate and speedy alerts. Several datasets were used to develop fatigue detection algorithms such as electroencephalogram (EEG), electrooculogram (EOG), electrocardiogram (ECG), and electromyogram (EMG) recordings of the driver's activities e.g., DROZY dataset. This study proposes a fatigue detection system based on Fast Fourier Transform (FFT) and Discrete Wavelet Transform (DWT) with machine learning and deep learning classifiers. The FFT and DWT are used for feature extraction and noise removal tasks. In addition, the classification task is carried out on the combined EEG, EOG, ECG, and EMG signals using machine learning and deep learning algorithms including 1D Convolutional Neural Networks (1D CNNs), Concatenated CNNs (C-CNNs), Support Vector Machine (SVM), Random Forest (RF), Decision Tree (DT), *k*-Nearest Neighbor (KNN), Quadrature Data Analysis (QDA), Multi-layer Perceptron (MLP), and Logistic Regression (LR). The proposed methods are validated on two scenarios, multi-class and binary-class classification. The simulation results reveal that the proposed models achieved a high performance for fatigue detection from medical signals, with a detection accuracy of 90% and 96% for multiclass and binary-class scenarios, respectively. The works in the literature achieved a maximum accuracy of 95%. Therefore, the proposed methods outperform similar efforts in terms of detection accuracy.

Keywords: deep learning; machine learning; drowsiness detection; medical signal classification; driver fatigue detection; feature extraction; FFT; DWT

Citation: Sedik, A.; Marey, M.; Mostafa, H. WFT-Fati-Dec: Enhanced Fatigue Detection AI System Based on Wavelet Denoising and Fourier Transform. *Appl. Sci.* **2023**, *13*, 2785. https://doi.org/10.3390/app13052785

Academic Editors: Tsung-Jung Liu and Kuan-Hsien Liu

Received: 17 January 2023
Revised: 6 February 2023
Accepted: 12 February 2023
Published: 21 February 2023

1. Introduction

Researchers in the automotive industry are currently working on a slew of drowsiness detection systems to address the widespread problem of drivers nodding off behind the steering wheel. Consider the various sensors, cloud services, servers, smartphones, and centralized and distributed data processing that comprise the Internet of Things and its associated applications [1]. Human behavior, automotive, and environmental analysis are the three most common approaches to developing an efficient fatigue detection system [2]. Figure 1 summarizes the key characteristics shared by these types of systems.

The first trend comprises behavioral technologies which employ image processing and computer vision to analyze the driver's images and videos. This method relies on monitoring many driver-related metrics to determine whether he is alert, tired, or asleep. Key factors are gleaned from observations such as yawning with the lips open and closed, eye closure, facial features, head posture, and nodding [3].

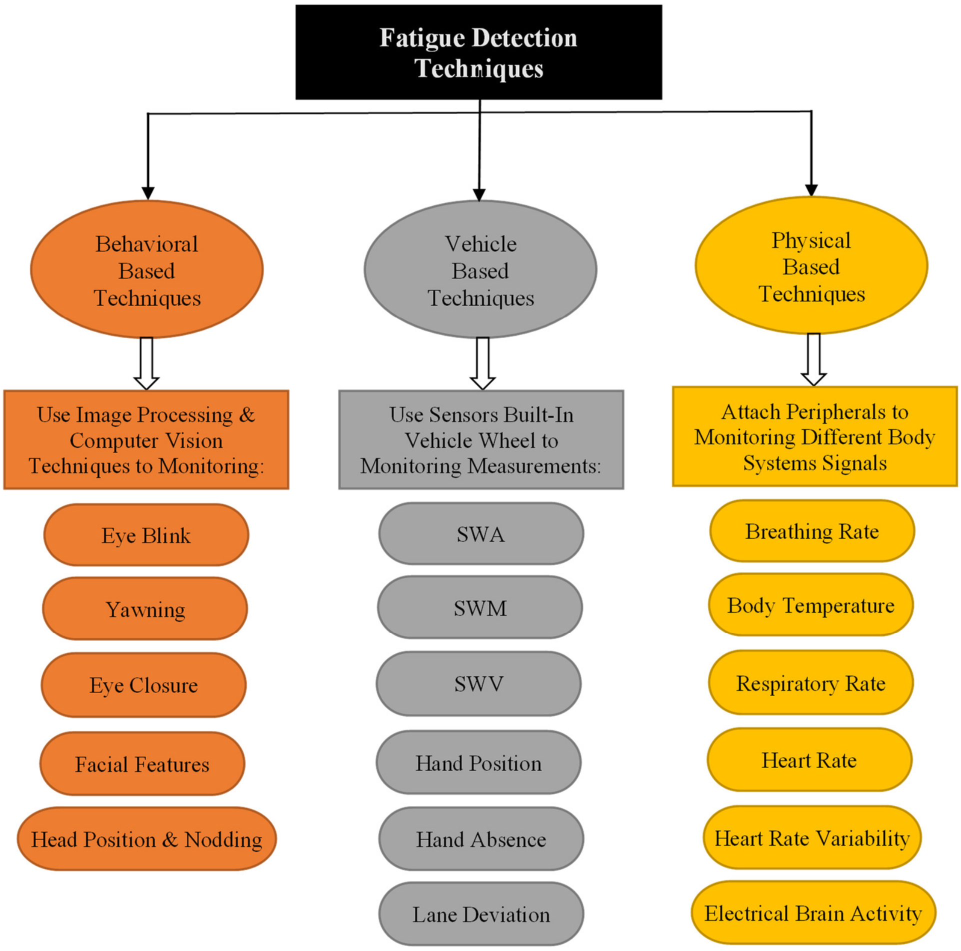

Figure 1. A summary of the major techniques used in fatigue detection systems.

In vehicle-based systems, devices and sensors are embedded in vehicle wheels which form a system for detecting driver fatigue [4]. This integrated system monitors steering wheel angle, steering wheel movement, steering wheel velocity, hand placement, hand absence, and lane departure.

Physical-based methods monitor the signals from the driver's internal systems by attaching sensors to the driver's hands, head, fingers, and chest, such as ECG, EOG, EEG, and percentage of eyelid closure (PERCLOS). In addition, monitoring various output signals [5], such as respiratory rate, core temperature, electrical brain activity, pulse rate, heart rate variability, and total heart rate, are used in this method.

Moreover, drowsiness detection system methods can be divided into traditional and machine learning algorithms [6]. SVM and CNN are widely used and highly efficient classifiers in machine learning algorithms [7]. SVM is accurate when it is applied to large datasets, but it suffers from low speed. On the other hand, CNN provides high accuracy and consistency across large and small datasets, but it takes time to train on CPUs and it is expensive to process on GPUs [7].

Developing a system to detect driver fatigue, with safe driving practices, is a significant undertaking. Previous attempts at behavior-based techniques involved evaluating images captured of the driver in real-time using Infrared (IR) illumination, then using software to track their driving behavior [8]. This concept uses a wide range of parameters including the PERCLOS, the number of times the driver nods his head, and how long he keeps his eyes closed. A fuzzy classifier examines these factors to determine whether the driver is in danger. The superiority of the system, over competing algorithms, is due to the abundant tracking, analysis factors, and day-and-night data collection periods.

A fatigue detection system was proposed by Flores et al. [9], which scanned and monitored the driver's face and eyes to decide based on facial expressions and eye movement. The gadget was tested in real-world scenarios with varying levels of illumination. Another method is proposed by Abtahi et al. [10] They created a straightforward technique based on image processing. Their strategy is to keep an eye out for signs of fatigue by tracking the driver's face in the image and capturing features like eye and lip movement to detect yawning and ocular languor. This method represents the wide variety of facial structures used while motoring. Other methods for improving the accuracy of fatigue detection include [11–13], which both seek to identify the similarity of geometrical features.

Physical-based fatigue detection comprises classifying medical signals. Some researchers employ different feature extraction algorithms such as Correa et al. [14], who used time and frequency characteristics extracted from EEG recordings. They stated that their Artificial Neural Network (ANN)-based classification system had an accuracy of 83%. Another feature extraction method using Approximation Entropy (AE) and Sample Entropy (SE) was applied to EEG signals by Xiong et al. [14] to predict driver fatigue. This method was carried out on fifty people. They used the SVM for classification, and their proposed method achieved a classification accuracy of 90% with two categories of driver weariness. Furthermore, driver fatigue was predicted using EEG data by Chai et al. [15] using an autoregressive model. In this study, 48 people participated with two fatigue levels. They employed Independent Component Analysis (ICA) to reduce the feature vector size as part of their investigation. They deployed a Bayesian classifier which achieved an accuracy of 88.2%. Another type of feature extraction from EEG signals based on Fuzzy Entropy (FE) is proposed by Yin et al. [16] They tested their method on six participants to identify two distinct states of driving fatigue using an ANN classifier which is reported to be 90%. Hu et al. [17] used AE, SE, and FE to extract the features from EEG data to evaluate driver fatigue. In their study, eight people volunteered to be assessed using an AdaBoost classifier with 92% accuracy. Min et al. [18] used the AE, SE, and FE which extracted features of EEG signals to identify fatigue. Their sensitivity, specificity, and accuracy for classifying data were all 100% when using the ANN classifier.

Trigonometric transformation techniques are involved in feature extraction. Ko et al. [19] extracted Frequency information from EEG signals using the FFT to detect the driver's state of weariness. Fifty participants used Virtual Reality (VR) equipment during the trials. According to proponents, the LR model reliably classified data at a 90% rate. Another effort is proposed by Wang et al. [20] to extract components from EEG recordings and they used Power Spectral Density (PSD) to perform this task. Their classification accuracy is 83% using the LR model. Mou et al. [21] used FFT to extract frequency information from EEG recordings to distinguish between two states of driver fatigue. They analyzed data from twenty individuals with a reliability in classifying objects of 85%. Nugraha et al. [22] extracted numerous time-frequency and statistical metrics from EEG data, such as mean, standard deviation, and correlation with FFT, to determine whether or not a driver was fatigued. Thirty people were tested using the Emotiv EPOC+ (EEG based device "https://www.emotiv.com/epoc/" (accessed on 29 November 2022)) to identify two distinct phases of driver fatigue. They boast a 96% accuracy rate when it enrolled into a classification task.

Another approach is proposed by Luo et al. [23]. They used a combination of adaptive scaling factor and entropy characteristics using two channels of EEG signals (Fp1 and Fp2). They achieved 40% on a two-stage classification of driver fatigue. In addition, the EEG toolbox was also used to filter out unwanted EOG activity. This task enhanced the system's performance with a classification accuracy of 98%.

Gao et al. [24] turned to deep neural networks (DNNs) with testing on ten participants. They used 11 convolutional layers to create their deep network. They achieved a classification rate of 95%. A combination of EEG signals, facial expressions, and gyroscope data is proposed by Karuppusamy et al. [25]. They proposed a system based on DNNs, which achieved an accuracy of 93%.

It is clear from the works discussed that many feature extraction methods were employed to extract the key features from the input signals. Furthermore, the classification task utilized several strategies to reach the optimal detection accuracy. However, they reached a maximum detection accuracy of 95% using powerful feature extractors and classifiers. As a result, this article attempts to build an improved system with a high detection accuracy rather than the ones proposed in the literature.

Machine and deep learning modalities have recently been involved in several applications [26,27], such as emotion recognition [28], speech recognition [29], and medical diagnosis [30–33]. In this paper, we propose a drowsiness detection system to determine the level of fatigue based on EEG, EOG, and EMG signals. The objective is to develop a system that can detect a driver's fatigue with a high detection rate and a fast testing time. For this purpose, we employed wavelet transform for the feature extraction task with PCA preprocessing. In addition, machine and deep learning models are deployed on the extracted features to detect fatigue states. The following are some examples of how the proposed work will advance the field:

1. Propose a feature extraction method based on trigonometric transformations for EEG signals.
2. Medical signal preprocessing using PCA and rescaling techniques.
3. Investigate an enhanced method for fatigue detection from EEG signals based on machine and deep learning models.
4. Evaluate the methods, discuss the results and highlight their advantages and disadvantages.
5. Compare the accomplished performance with the works in the literature.

The remainder of this paper is divided into four sections. Section two describes the materials and methods proposed for this work. The third section discusses the outcomes of the proposed methods. Section four briefly compares the proposed methods to works in the literature. Finally, section five brings the paper to a close.

2. Materials and Methods

This paper proposes a fatigue detection system based on medical signals. The proposed method is divided into four stages: feature extraction, preprocessing, scaling, and classification, as shown in Figure 2. The feature extraction task is carried out using DWT, FFT, Discrete Cosine Transform (DCT), and Discrete Sine Transform (DST). The DWT is employed for noise reduction. The extracted signals are transformed using the trigonometric transformations, FFT, DCT, and DST. PCA is used through the preprocessing stage to improve the classification process and decorrelate the extracted features. The extracted features are then classified using machine and deep learning models.

Classifiers such as DT, KNN, SVM, RF, MLP with backpropagation, QDA, and LR are used in the machine learning approach. In addition, the hyperparameters of the proposed algorithms are mechanically chosen using the grid search method [34,35]. Table 1 illustrates samples of the ittrations of hyperparameter selection, while Table 2 presents the results of our research regarding the optimal values for the classifier's hyper-parameters.

The deep learning approach includes concatenated CNNs and 1D CNNs. The proposed CNN model consists of an input layer, three convolutional, max pooling, dropout, and batchnormalization layers, a flatten layer, and a dense layer. At the input layer, the data is reduced to 500 features to be enrolled in the proposed models. The maximum pooling and convolutional layers are used to extract features from input data. The first, second, and third convolutional layers have 128, 128, and 256 filters, respectively. Each set also includes a dropout and a batch normalization layer. These layers are used to prevent overfitting from occurring. Furthermore, the flatten layer, which prepares the feature vectors for enrollment in classification, completes the connection between the feature extractors and the classification layer. A dense layer with a softmax activation function is used to deploy the classification task.

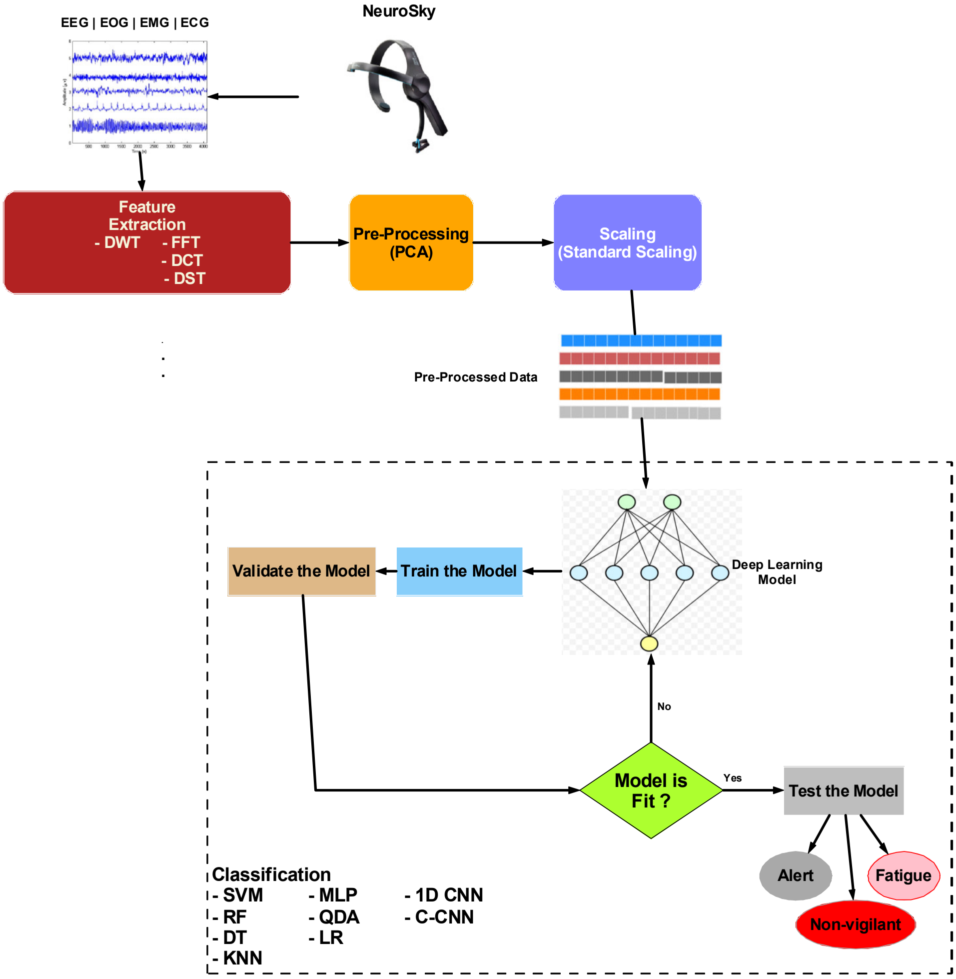

Figure 2. Proposed system for detecting fatigue.

Table 1. Sample of iterations for Hyperparameter Optimization.

Hyper Parameter						Accuracy
No. of Filters	**Activation Function**	**Dropout**	**Epochs**	**Learning Rate**	**Optimizer**	
128	relu	0.4	150	0.01	adam	1
256	relu	0.2	200	0.001	rmsprop	1
256	relu	0.3	150	0.01	adam	1
256	relu	0.2	150	0.001	rmsprop	0.99900794
64	relu	0.3	150	0.01	rmsprop	0.99900794
256	relu	0.2	200	0.01	rmsprop	0.99900794
128	relu	0.3	200	0.01	adam	0.99900794
256	relu	0.2	150	0.001	adam	0.99900794
64	relu	0.4	100	0.001	rmsprop	0.991071403
64	relu	0.4	150	0.001	adam	0.990079343
64	relu	0.3	100	0.01	adam	0.990079343
64	relu	0.4	100	0.01	adam	0.989087284
256	relu	0.4	100	0.001	adam	0.988095224
256	relu	0.2	100	0.001	adam	0.987103164
256	relu	0.3	200	0.01	adam	0.986111104
56	56	75	96	52	56	72
59	68	88	91	57	62	65
50	54	18	77	71	59	34

Table 2. Hyperparameters of The Proposed Methods.

Model	Hyperparameters
SVM	C: 275 gamma: 'scale' kernel: 'rbf'
RF	n_estimators:79 Criterion: 'entropy'
DT	criterion: 'gini' min_samples_leaf: 1 min_samples_split: 2 ccp_alpha: 0
KNN	n_neighbors:1 leaf_size: 30 metric: 'minkowski' p: 2 weights': 'uniform'
QDA	tol = 0.0001
MLP	Num_hidden_layers:2 hidden_layer_sizes: [34,35] activation: 'relu' max_iter: 200 solver: 'adam'
LR	solver: 'lbfgs' C: 1.0 fit_intercept: True
CNN	Optimizer: adam Epochs: 150 Batch size: 20 Activation function: relu Number of filters: 128 Dropout: 0.4 Learning rate: 0.01
C-CNN	Optimizer: adam Epochs: 150 Batch size: 20 Activation function: relu Number of filters: 128 Dropout: 0.4 Learning rate: 0.01

In this paper, we propose another sequential model based on C-CNNs. Concatenation describes how multiple forks or sub-models process the input data. In a concatenation layer, the results of these individual models are combined. The proposed concatenated model's architecture, as shown in Figure 3, consists of an input layer, and two branches of a sequence of convolutional, max pooling, and dropout layers. The branch outputs are then concatenated using a concatenation layer. The concatenated feature vector is then enrolled in three convolutional, max pooling, and dropout layers. A flatten layer is used for fully connected tasks, and a dense layer is used for classification tasks. Figure 4 depicts the hyperparameters of the proposed C-CNN model.

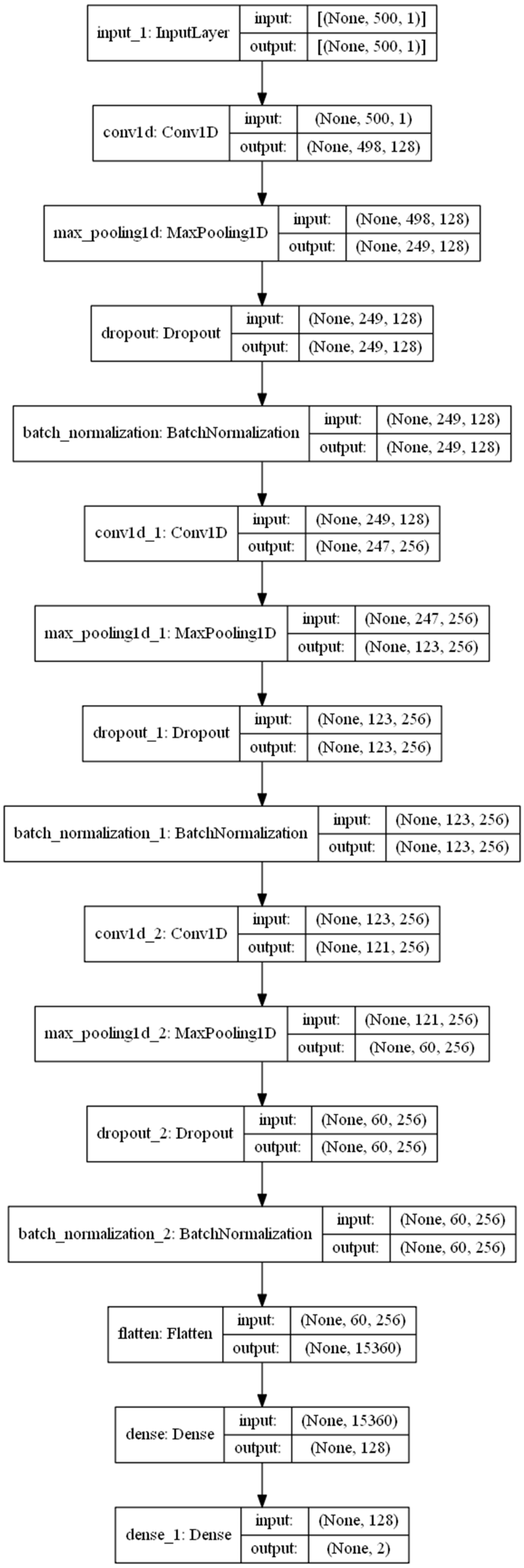

Figure 3. Architecture of the proposed 1D CNN model.

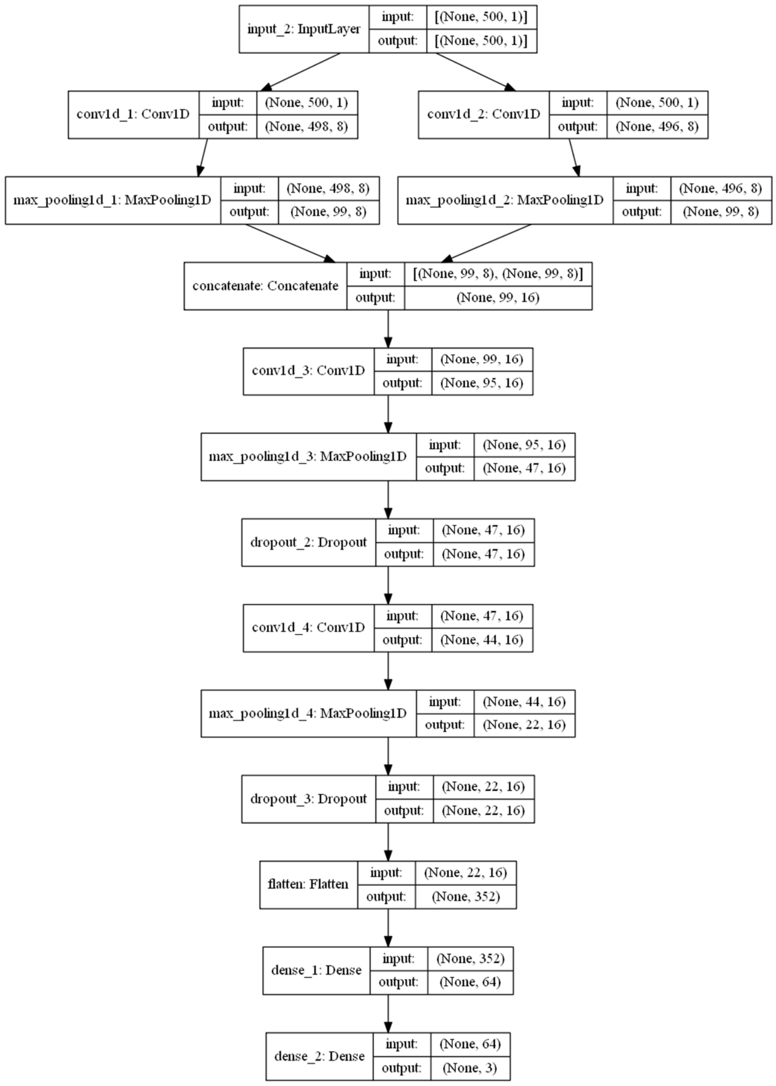

Figure 4. Architecture of the proposed C-CNN model.

3. Results

This section provides a thorough examination of the proposed algorithms. First, the dataset is thoroughly described. The evaluation metrics used to assess the performance of the proposed methods are displayed. The hyperparameter selection is discussed. The findings are then summarized, followed by commentary and discussion. The results are then compared to those found in the literature.

The proposed methods are performed on a PC outfitted with a Core i7 processor, an 8 GB NVIDIA GPU device, 32 GB of RAM, and Windows 11. The proposed models are deployed using Python 3.8 codebases using the Keras, Scikit-learn, and TensorFlow libraries. The proposed methods' layers and learning parameters are displayed in Table 2 and Figures 3 and 4.

3.1. Dataset Description

The proposed techniques are tested on the "ULg Multimodality Drowsiness Database" (abbreviated DROZY [36]). This dataset is in two parts (video monitoring and EEG signals). First, data from 14 healthy young adults were gathered (3 males and 11 females).

DROZY includes a sleepiness indicator that uses data from sources such as the Karolinska Sleepiness Scale (KSS) and polysomnography (PSG) to provide an accurate picture of a person's sleepiness. Polysomnograms typically have eleven electrodes: five for EEG, two for EOG, one for EMG, and one for ECG, all of which operate at 512 hertz. Figure 5 depicts the progression of polysomnographic signals through the driver's brain, using what is now known as NeuroSky (NeuroSky. NeuroSky is an EEG and ECG biosensor for consumer-facing, wearable technology products (https://neurosky.com/ accessed on 30 September 2022)).

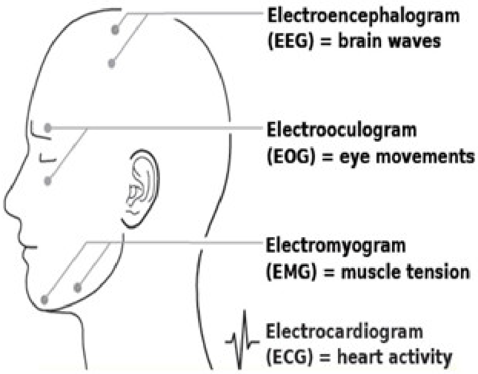

Figure 5. The physical distribution of drozy polysomnography signals on the driver's head.

3.2. Evaluation Metrics

To rank the quality of the proposed solutions, various metrics are used. The F1-Score is based on the metrics of Recall, Precision, F1-score, Accuracy, and Matthews Correlation Coefficient (MCC). The corresponding equations define the measurements from Equations (1)–(5) [37–39].

Where:

(1) The number of sleepy states that were incorrectly labeled "normal" is shown in the false-negative column.
(2) The True Positive metric indicates the percentage of drowsy states that were accurately identified.
(3) The True Negative () value indicates the proportion of false negatives correctly identified as false positives.
(4) The number of times a normal status was mistakenly labeled as a drowsy status is shown in the false positive.

$$Accuracy = \frac{No.of\ correctly\ detected\ images}{Total\ No.of\ images} \times 100 = \frac{(T_N + T_P)}{(T_P + F_P + T_N + F_N)} \times 100 \quad (1)$$

$$Recall = TPR = T_P/(T_P + F_N) = (1 - FNR) \quad (2)$$

$$precision = T_P/(T_P + F_P) \quad (3)$$

$$F1 = 2 \times ((precision \times recall)/(precision + recall)) \quad (4)$$

$$MCC = \frac{(T_P \times T_N) - (F_P \times F_N)}{\sqrt{((T_P + F_P) \times (T_P + F_N) \times (T_N + F_P) \times (T_N + F_N))}} \times 100 \quad (5)$$

3.3. Hyperparameter Setting

The process of hyperparameter selection is carried out using a grid search algorithm for both machine learning and deep learning approaches to select the optimal values which achieve the maximum accuracy. Table 2 shows the hyperparameters which are set to the proposed methods. These hyperparameters are achieved with 100 iterations for each model.

The strategy of hyperparameter selection is based on the permutations of model architecture and the training process. The model architecture trend comprises the values of filters of the convolutional layers, units of the dropout layers, and activation functions. The training process trend comprises the type of optimizer, learning rate, and number of epochs. Figures 6 and 7 show samples of the learning curve for accuracy and loss which is obtained during the hyperparameter optimization. It can be observed that the performance of the model is enhanced through the runs due to the permutations of the hyperparamer values. In addition, Figure 8 shows an infograph of the accuracy with the variation of hyperparameter values. Moreover, Table 1 illustrates some iterations for the hyperparamer optimization for the deep learning model. Table 2 illustrates the selected hyperparameters for the proposed methods.

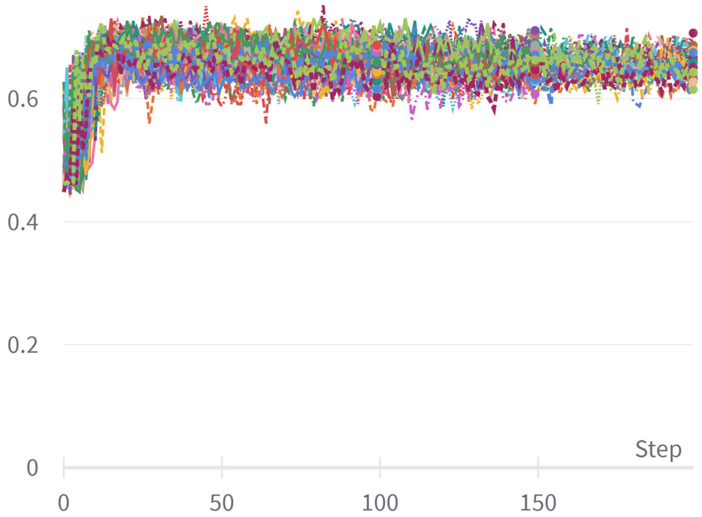

Figure 6. Learning curves (accuracy) of the iterations in the hyperparameter optimization.

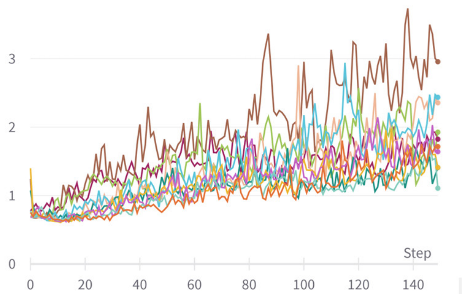

Figure 7. Learning curves (loss) of the iterations of the hyperparameter optimization.

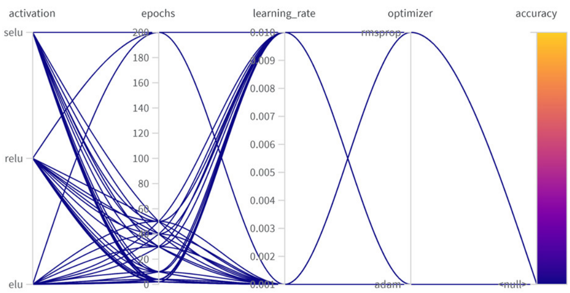

Figure 8. Infograph of the variation of the hyperparameters and the accuracy.

3.4. Simulation Results

This section discusses the simulation results of the proposed methods for different feature extractions and classification techniques. The strategy to propose an efficient system comprises the selection of a strong feature extraction technique, then the selection of an efficient classification method. This paper selects the feature extraction technique among DWT, FFT, DWT with FFT, DCT, DCT with DWT, DST, and DST with DWT. This variety of feature extraction methods provides an extensive study to achieve the optimal one. In addition, these techniques are evaluated prior to precision, recall, F1-score, and accuracy using the proposed classification techniques. Tables 3–6 illustrates the evaluation metrics of the feature extraction techniques through the employment of the proposed classification methods. The simulation results reveal that FFT with DWT achieves the optimal performance among the presented methods.

Table 3. Brief Comparison among The Precision of The Proposed Machine Learning Models in Different Domains.

Scenario	Model	Feature Extraction Method							
		Time Domain	Time Domain + DWT	FFT	FFT + DWT	DCT	DCT + DWT	DST	DST + DWT
Multiclass	SVM	41	50	89	87	50	50	48	48
	RF	47	56	84	89	49	46	42	48
	DT	38	42	67	73	32	41	47	29
	KNN	43	51	82	90	38	38	34	34
	QDA	37	44	84	88	36	33	35	41
	MLP	39	40	82	87	42	44	48	44
	L.R.	43	43	86	90	40	44	49	41
	CNN	43	52	71	79	42	47	53	43
	C-CNN	34	56	28	47	30	18	20	44
Binary-Classes	SVM	41	57	77	97	63	63	68	68
	RF	58	67	83	96	68	65	61	67
	DT	53	57	82	82	41	50	66	48
	KNN	47	55	70	92	53	53	51	51
	QDA	47	54	69	92	57	54	42	48
	MLP	51	52	64	93	57	59	63	59
	L.R.	56	56	75	96	52	56	72	64
	CNN	59	68	88	91	57	62	65	55
	C-CNN	50	54	18	77	71	59	34	48

Table 4. Brief Comparison among The Recall of The Proposed Machine Learning Models in Different Domains.

Scenario	Classifier	Feature Extraction Method							
		Time Domain	Time Domain + DWT	FFT	FFT + DWT	DCT	DCT + DWT	DST	DST + DWT
Multiclass	SVM	41	50	84	87	47	49	48	48
	RF	45	55	83	89	48	46	45	42
	DT	37	41	66	73	32	40	38	47
	KNN	36	44	81	85	32	35	34	34
	QDA	36	43	75	87	36	40	38	35
	MLP	39	40	82	87	41	44	46	48
	L.R.	42	42	86	90	39	44	45	49
	CNN	43	52	69	79	42	47	47	52
	C-CNN	33	37	27	48	30	18	30	18
Binary-Classes	SVM	48	57	68	96	61	63	65	65
	RF	57	67	83	96	67	65	63	60
	DT	53	57	82	82	42	50	57	66
	KNN	47	55	70	91	49	52	51	51
	QDA	47	54	59	89	46	50	45	42
	MLP	51	52	64	93	55	58	61	63
	L.R.	56	56	71	96	51	56	67	71
	CNN	59	68	88	89	57	62	60	65
	C-CNN	50	54	18	51	71	59	34	48

Table 5. Brief Comparison among The F1-score of The Proposed Machine Learning Models in Different Domains.

Scenario	Classifier	Feature Extraction Method							
		Time Domain	Time Domain + DWT	FFT	FFT + DWT	DCT	DCT + DWT	DST	DST + DWT
Multiclass	SVM	39	58	84	86	45	48	47	47
	RF	44	55	84	89	48	46	45	42
	DT	37	41	66	73	32	40	38	47
	KNN	34	43	81	85	26	32	34	34
	QDA	37	44	73	87	36	31	30	27
	MLP	38	39	82	87	41	44	45	47
	L.R.	42	42	86	90	39	44	45	49
	CNN	43	51	70	78	42	46	46	51
	C-CNN	32	36	29	47	30	22	29	17
Binary-Classes	SVM	38	57	65	96	60	63	63	63
	RF	56	67	83	96	67	65	62	59
	DT	53	57	82	82	42	50	57	66
	KNN	44	53	70	91	46	52	48	48
	QDA	47	54	53	90	59	54	45	42
	MLP	51	52	64	93	55	58	61	63
	L.R.	56	56	69	96	51	56	67	71
	CNN	59	67	88	90	58	62	60	65
	C-CNN	50	54	17	64	66	58	34	48

Table 6. Brief Comparison among The Accuracy of The Proposed Machine Learning Models in Different Domains.

Scenario	Classifier	Feature Extraction Method							
		Time Domain	Time Domain + DWT	FFT	FFT + DWT	DCT	DCT + DWT	DST	DST + DWT
Multiclass	SVM	41	50	84	86	47	49	48	48
	RF	45	55	83	89	48	46	45	42
	DT	37	41	66	73	32	40	38	47
	KNN	36	43	81	84	32	35	34	34
	QDA	36	43	75	87	36	33	38	35
	MLP	39	40	82	87	41	44	46	48
	L.R.	42	42	86	90	39	44	45	49
	CNN	43	51	69	78	42	47	47	52
	C-CNN	33	37	27	48	30	18	30	18
Binary-Classes	SVM	48	57	68	96	61	63	65	65
	RF	57	67	83	96	67	65	63	60
	DT	53	57	82	83	42	50	57	66
	KNN	47	54	70	91	49	52	51	51
	QDA	47	54	59	90	57	54	45	42
	MLP	51	52	64	93	55	58	61	63
	L.R.	56	56	71	96	51	56	67	71
	CNN	59	67	88	90	57	62	60	65
	C-CNN	50	54	18	64	45	59	34	48

Moreover, the classification task is carried out using machine learning and deep learning approaches. The selection of classification method is carried out among the proposed methods including SVM, RF, DT, KNN, QDA, MLP, LR, CNN, and C-CNN. The optimal classification method is one which achieves a high performance prior to accuracy of detection. The proposed classification methods are carried out on the EEG signals in the time domain and the frequency domain. The performance of the proposed methods are evaluated prior to precision, recall, f1-score, and accuracy. The dataset is split into 70% and 30% for training and testing, respectively. In addition, these methods are trained and validated using k-fold cross validation, with k = 10. Furthermore, the classification task is performed in two scenarios of detection, binary-class and multi-class. The objective of the binary-class classification is to distinguish between states of alertness and tiredness. On the other hand, the objective of the multi-class classification is to classify among alert, tired, and non-vigilant states. The learning curves of the proposed machine learning methods are shown in Figures 9 and 10, while the visual representation of the confusion matrices are shown in Figures 11 and 12. In addition, the learning curves of the deep learning are displayed in Figures 13 and 14. A visual representation of the confusion matrix of the proposed deep learning methods are shown in Figures 15 and 16. Table 7 illustrates the simulation results of the proposed classification methods which are carried out on the transformed EEG signals using FFT with DWT. In a multiclass scenario, the proposed LR and RF models outperform the others with 90% and 89% accuracy, respectively, while SVM, RF and LR have 96% accuracy, for the binary-class scenario. Therefore, the proposed system consists of FFT with DWT for feature extraction and a LR classifier for the wide deployment for both binary-class and multiclass scenarios.

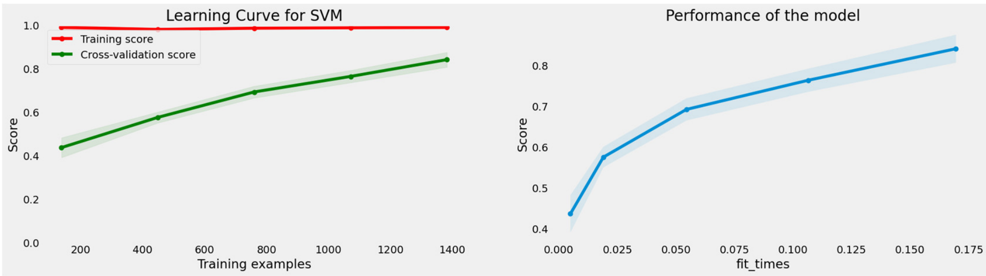

(**a**)

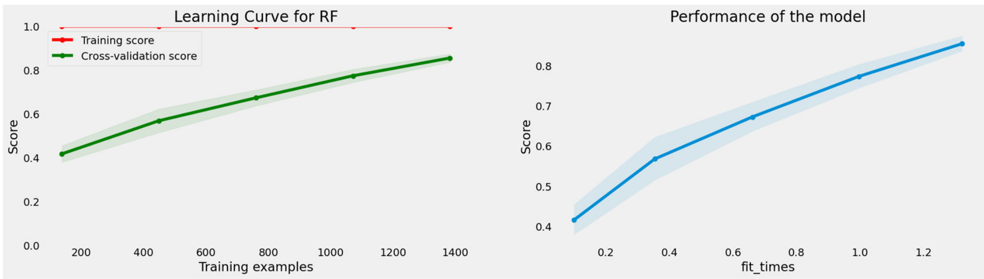

(**b**)

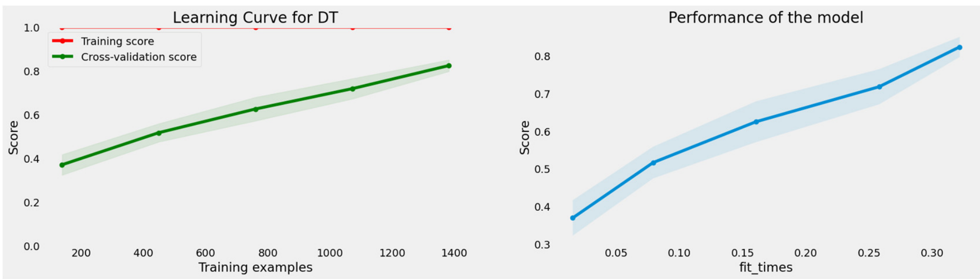

(**c**)

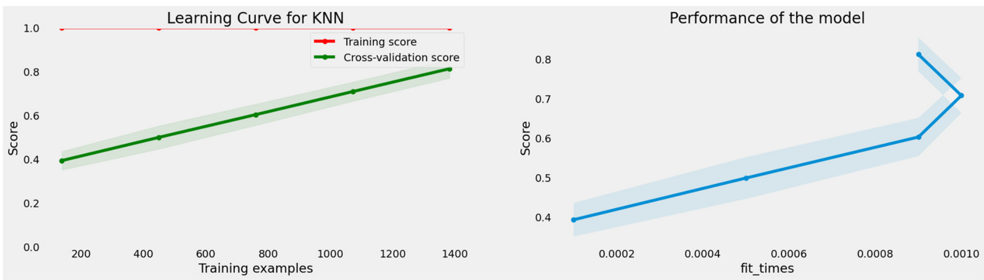

(**d**)

Figure 9. *Cont.*

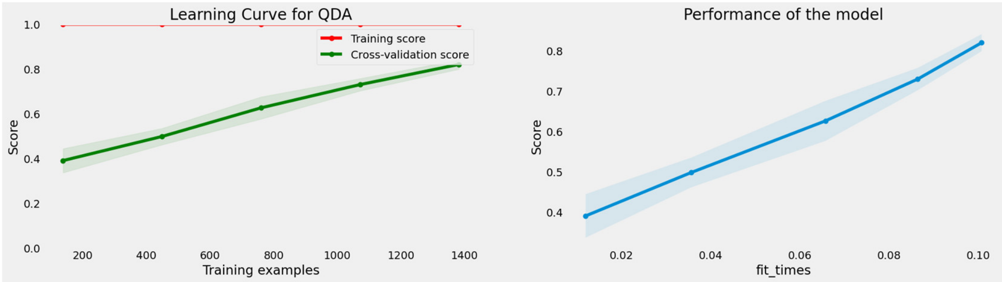

(**e**)

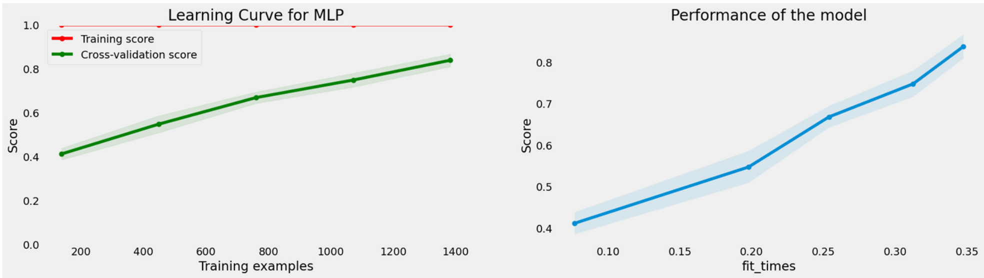

(**f**)

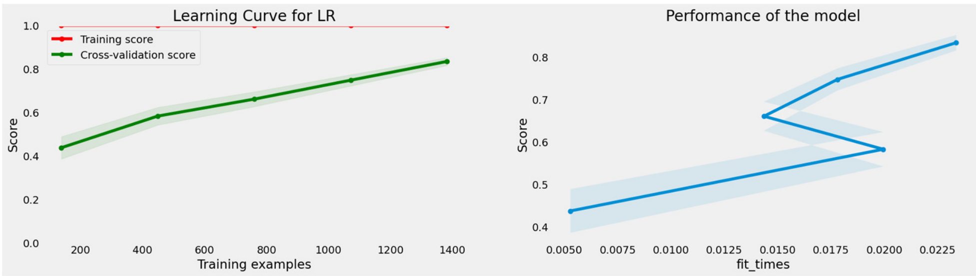

(**g**)

Figure 9. Multiclass learning and performance curves of the proposed machine learning models. (**a**) Learning Curve and Performance plots of The Proposed SVM Model. (**b**) Learning Curve and Performance plots of The Proposed RF Model. (**c**) Learning Curve and Performance plots of The Proposed DT Model. (**d**) Learning Curve and Performance plots of The Proposed KNN Model. (**e**) Learning Curve and Performance plots of The Proposed QDA Model. (**f**) Learning Curve and Performance plots of The Proposed QDA Model. (**g**) Learning Curve and Performance plots of The Proposed LR Model.

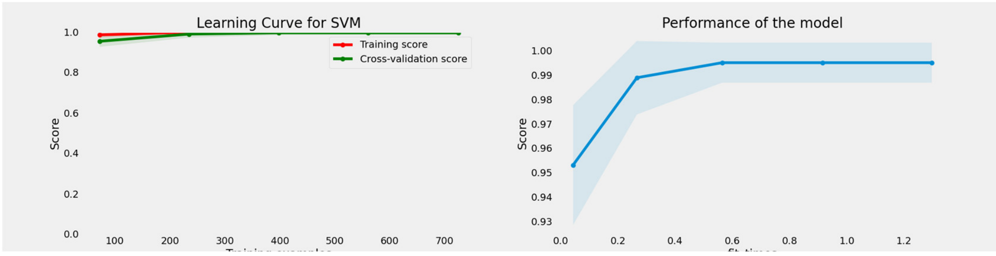

(**a**)

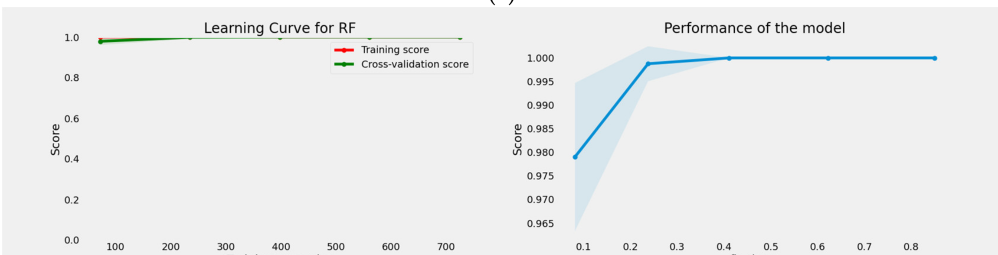

(**b**)

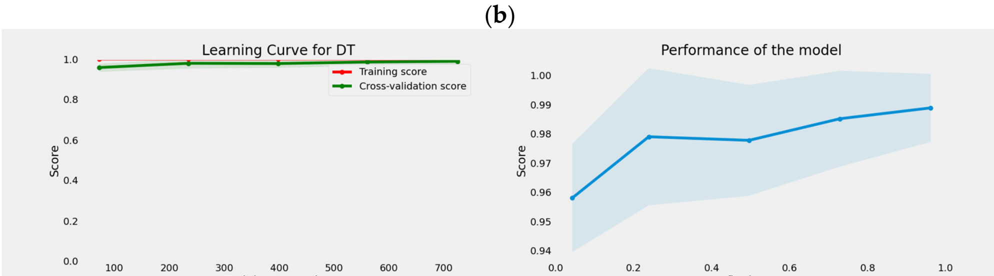

(**c**)

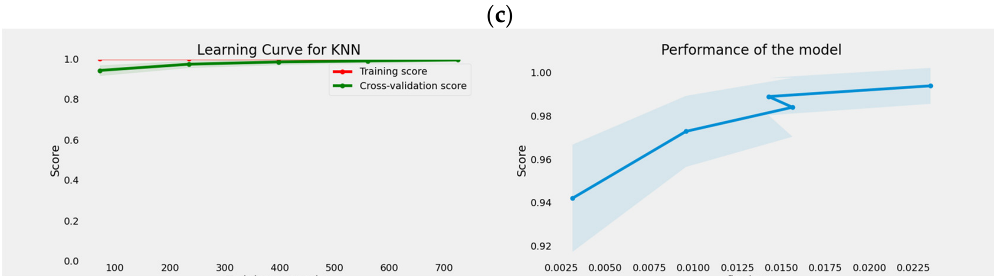

(**d**)

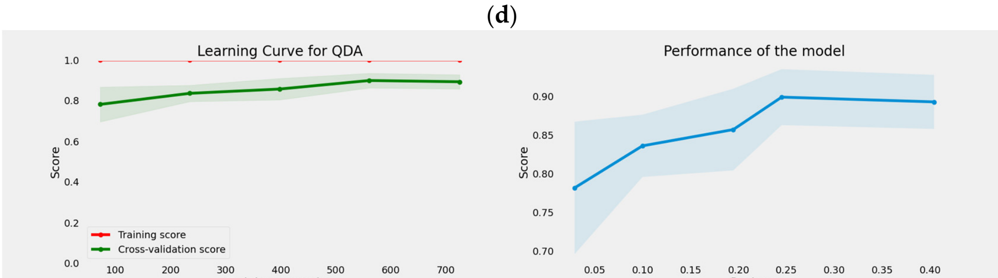

(**e**)

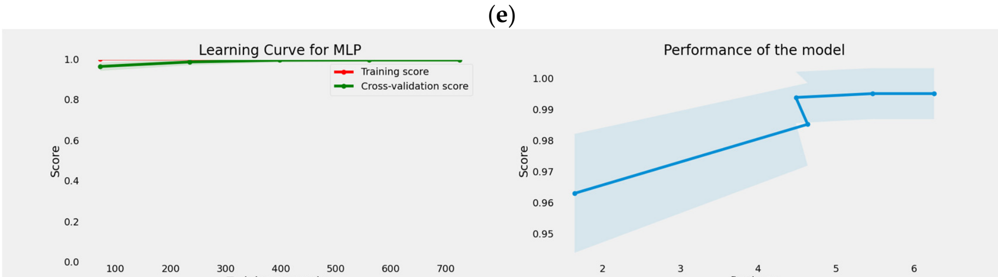

(**f**)

Figure 10. *Cont.*

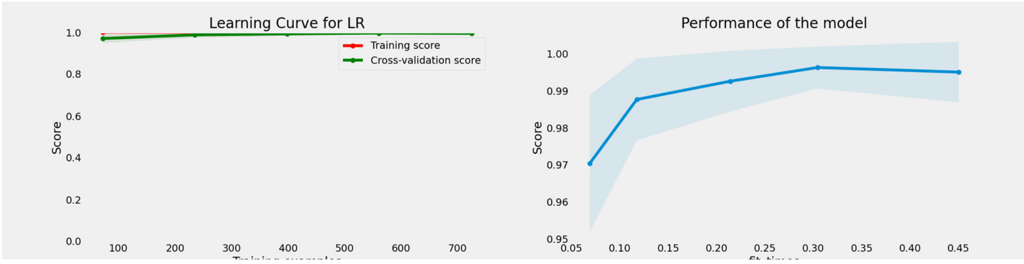

(**g**)

Figure 10. Binary-class learning and performance curves of the proposed machine learning models. (**a**) Learning Curve and Performance plots of The Proposed SVM Model. (**b**) Learning Curve and Performance plots of The Proposed RF Model. (**c**) Learning Curve and Performance plots of The Proposed DT Model. (**d**) Learning Curve and Performance plots of The Proposed KNN Model. (**e**) Learning Curve and Performance plots of The Proposed QDA Model. (**f**) Learning Curve and Performance plots of The Proposed MLP Model. (**g**) Learning Curve and Performance plots of The Proposed LR Model.

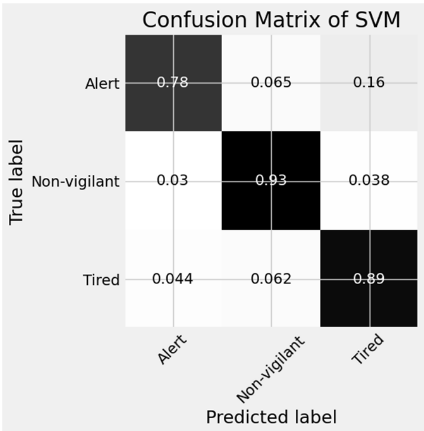

(**a**)

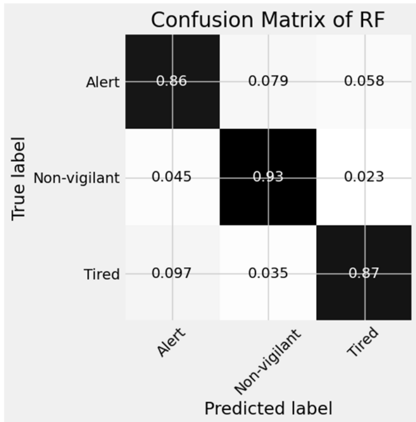

(**b**)

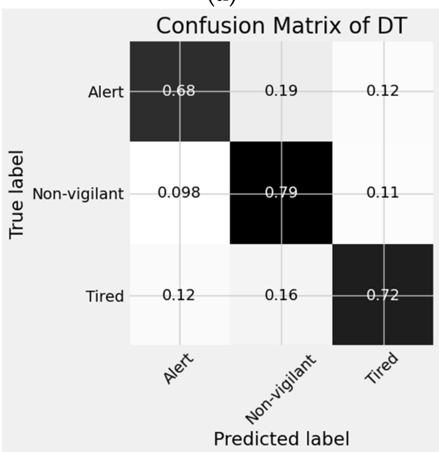

(**c**)

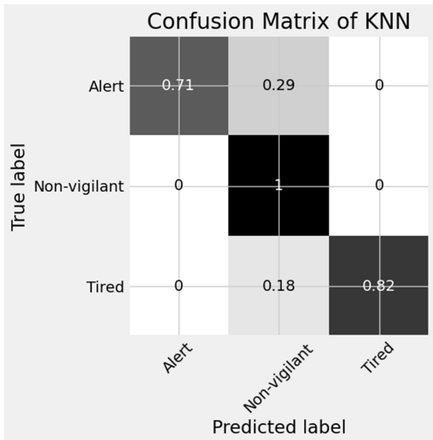

(**d**)

Figure 11. *Cont.*

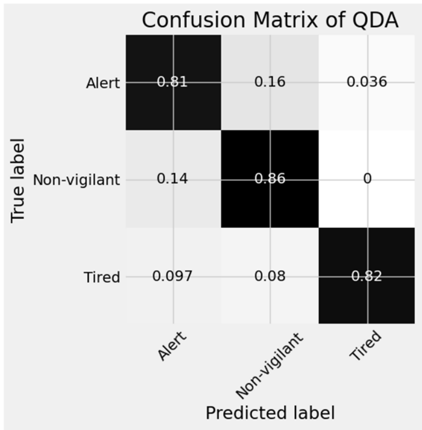

(**e**)

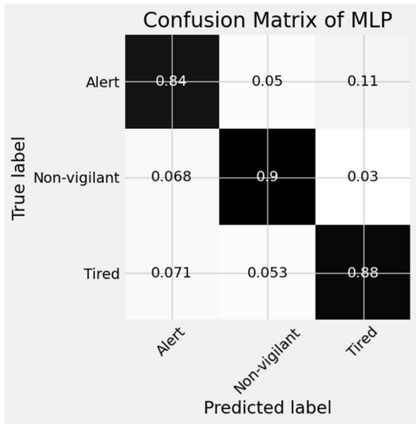

(**f**)

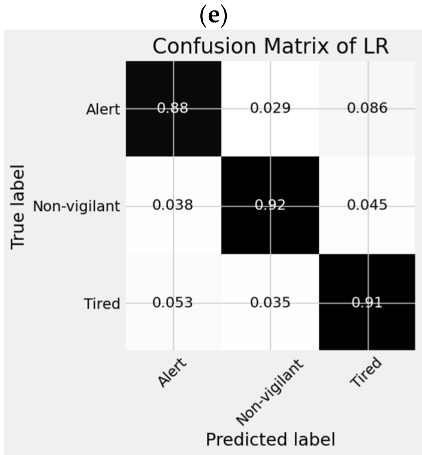

(**g**)

Figure 11. Confusion Matrix of The Proposed Machine Learning Models for *Multi*-class *Scenarion* (**a**) SVM, (**b**) RF, (**c**) DT, (**d**) KNN, (**e**) QDA, (**f**) MLP, (**g**) LR.

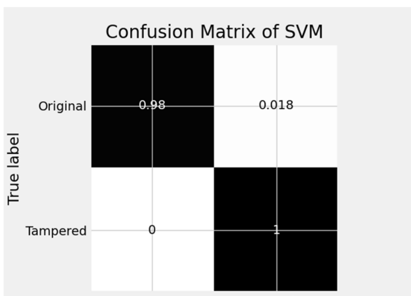

(**a**)

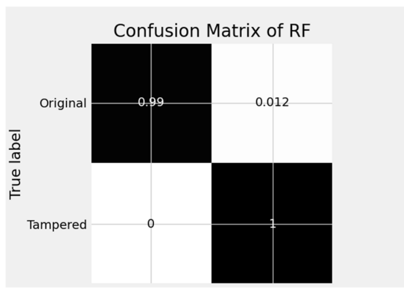

(**b**)

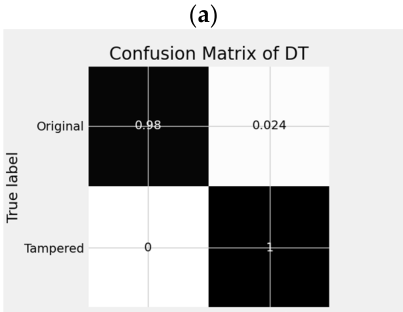

(**c**)

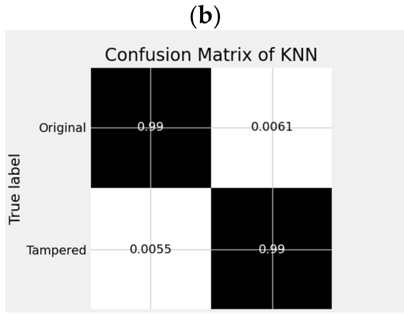

(**d**)

Figure 12. *Cont.*

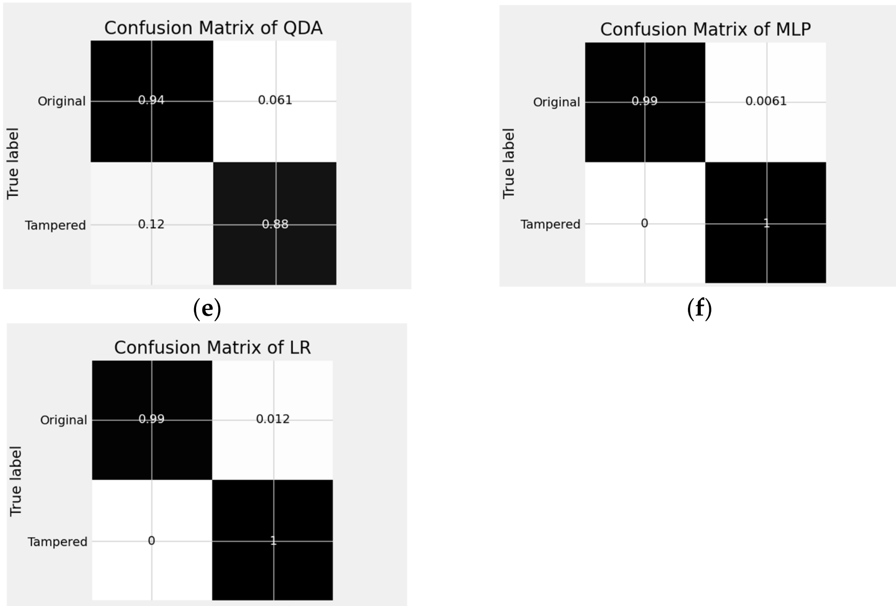

(e) (f)

(g)

Figure 12. Confusion Matrix of The Proposed Machine Learning Model for Binary Classification (**a**) SVM, (**b**) RF, (**c**) DT, (**d**) KNN, (**e**) QDA, (**f**) MLP, (**g**) LR.

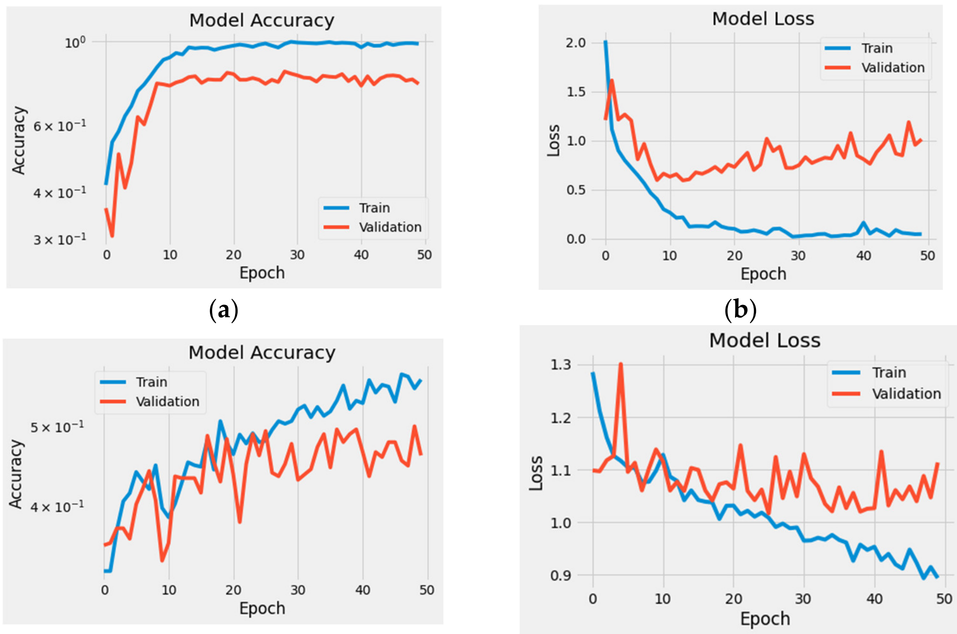

(a) (b)

(c) (d)

Figure 13. Proposed Deep Learning Models for Multi-class Scenario Learning and Performance Curves. (**a**) Accuracy of 1D CNN. (**b**) Loss of 1D CNN. (**c**) Accuracy of C-CNN. (**d**) Loss of C-CNN.

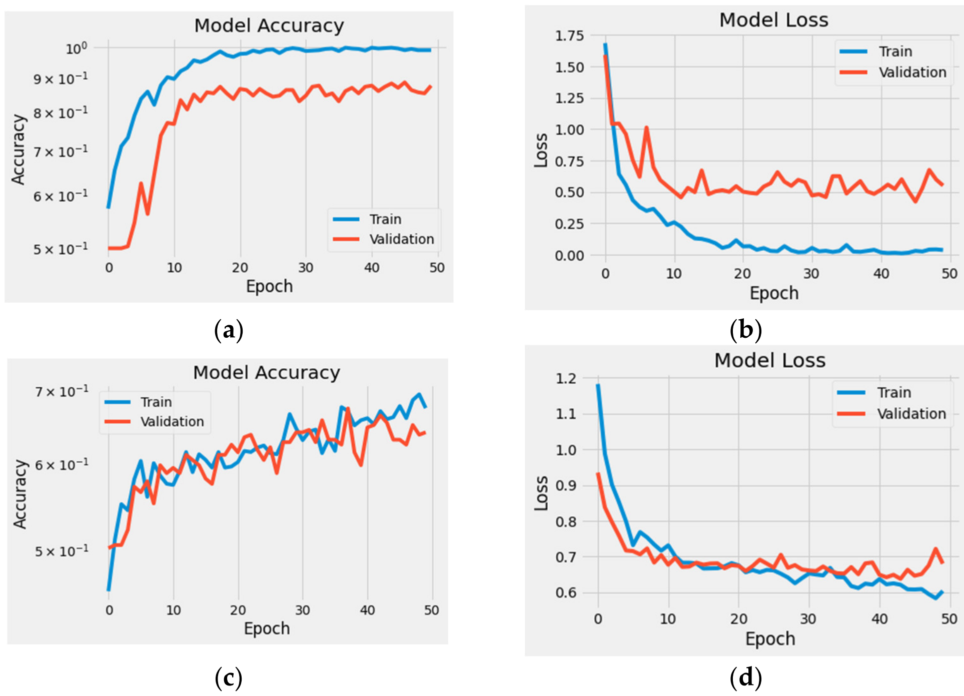

Figure 14. Deep learning models for binary-class scenario learning and performance curves (**a**) Accuracy for 1D CNN, (**b**) Loss for 1D CNN, (**c**) Accuracy for C-CNN, (**d**) Loss for C-CNN.

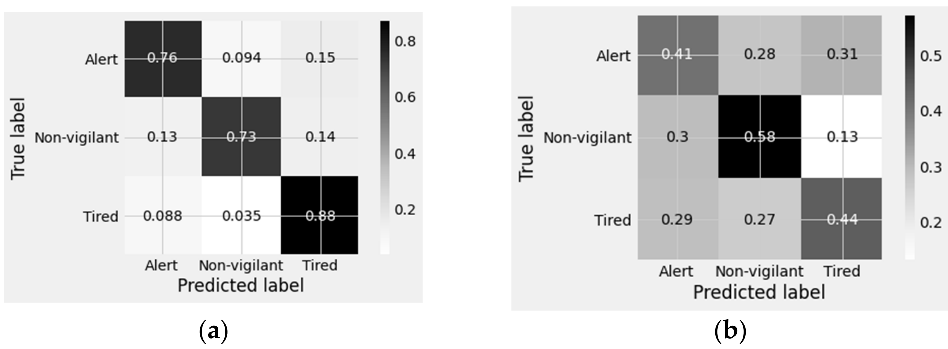

Figure 15. Confusion Matrix of The Proposed Deep Learning Model for Multi Classification. (**a**) iD CNN. (**b**) C-CNN.

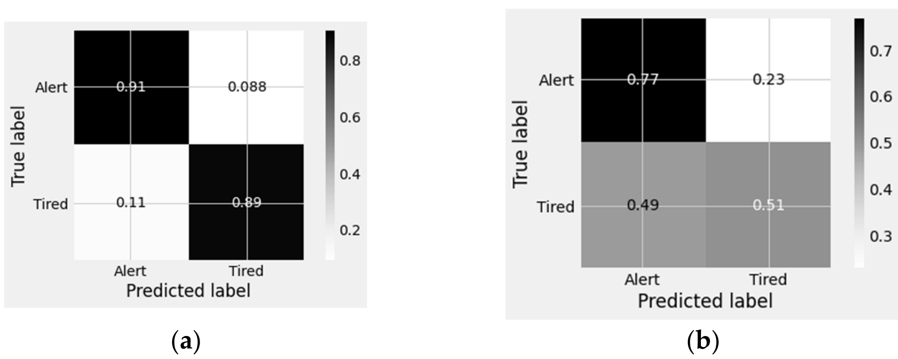

Figure 16. Confusion Matrix of The Proposed Deep Learning Model for Binary Classification (**a**) iD CNN. (**b**) C-CNN.

Table 7. Brief Comparison among The Proposed Machine Learning Models.

Scenario	Model	Precision	Recall	F1-Score	Accuracy	MCC
Multiclass	SVM	87	87	86	86	80
	RF	89	89	89	89	83
	DT	73	73	73	73	59
	KNN	90	85	85	84	79
	QDA	88	87	87	87	75
	MLP	87	87	87	87	81
	L.R.	90	90	90	90	86
	CNN	79	79	78	78	73
	C-CNN	47	48	47	48	42
Binary-Classes	SVM	97	96	96	96	93
	RF	96	96	96	96	92
	DT	82	82	82	83	65
	KNN	92	91	91	91	83
	QDA	92	89	90	90	81
	MLP	93	93	93	93	87
	L.R.	96	96	96	96	94
	CNN	91	89	90	90	82
	C-CNN	77	51	64	64	59

4. Discussion

This paper proposes a system for drowsiness detection based on medical signals. This system comprises feature extraction and classification tasks. The feature extraction task is carried out using several trigonometric transformations including DWT, FFT, DCT, and DST. The classification task is performed using machine learning and deep learning algorithms. Figure 17 shows the extracted features and their importance for the output. The accomplished system comprises FFT with DWT for feature extraction and LR for classification. In this section, we discuss the performance of the proposed system in different cases including the performance of the LR classifier on the signals in the time domain and different transformations in addition to its performance with the added DWT denoising technique. Figure 18 shows a comparison of the proposed system in different scenarios including binary-class and multi-class scenarios.

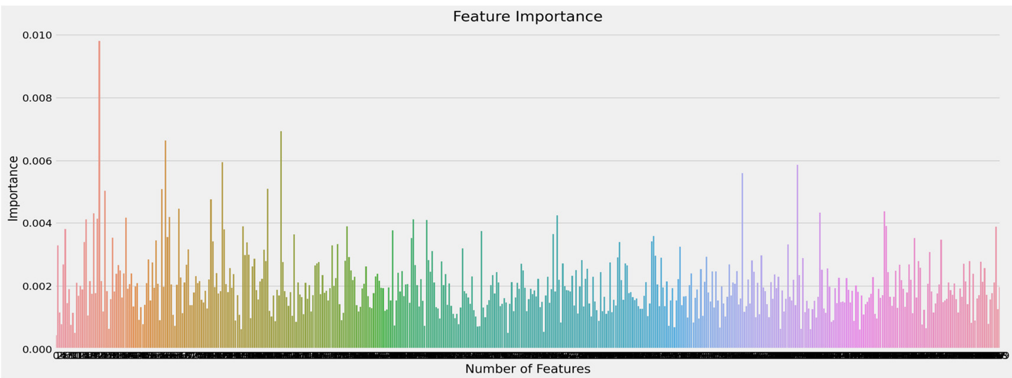

Figure 17. Plot of The Importance of The Input Features.

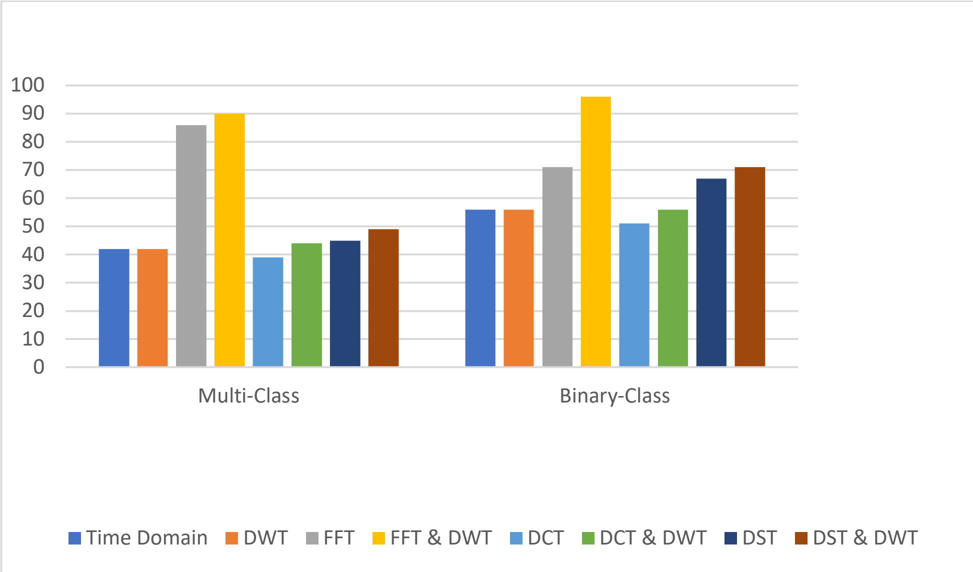

Figure 18. Brief Comparison of The Proposed System in different scenarios.

Moreover, the proposed models are compared with the efforts in the literature. This comparison comprises both feature extraction and classifications utility for each research work. Table 8 illustrates this comparison prior to accuracy of detection. Corea et al. [40] proposes a system based on multimodal analysis for feature extraction and ANN for classification. They achieved 83% accuracy of detection. Another work was proposed by Ko et al. [41] which used FFT for feature extraction and ANN for classification. They deployed their system on EEG signals from a wireless device, like Neurosky. They achieved an accuracy of detection of 90%. It can be observed that the employment of the DWT denoising technique and different classifiers leads to a considerable enhancement of the accuracy. Yin et al. proposed their system based on FE and SVM for feature extraction and classification tasks, respectively. They achieved an accuracy of detection of 95%. This comparison reveals that the proposed system presents a superior performance than the works in the literature. Therefore, it can be considered as an efficient fatigue detection system for real-life applications.

Table 8. Brief Comparison among The Proposed Models and Works in The Literature.

Work	Year	Feature Extractor	Classifier	Accuracy
Corea et al. [40]	2014	Multimodal Analysis	ANN	83
Ko et al. [41]	2015	FFT	ANN	90
Xiong et al. [14]	2016	AE and SE	SVM	90
Chai et al. [15]	2016	Entropy Rate Round Minimization Analysis	BNN	88.2
Yin et al. [16]	2017	FE	SVM	95
Karuppusamy et al. [25]	2020	DNN	DNN	73
Lui et al. [42]	2020	Deep Transfer Learning	Deep Learning	93
Proposed	2023	FFT + DWT	SVM	96
		FFT + DWT	RF	96
		FFT + DWT	LR	96

5. Conclusions

The problem of driver fatigue detection has been discussed in this paper. The proposed approach comprises both feature extraction and classification tasks. The feature extraction task has been accomplished using FFT and DWT. The classification task has been performed using machine learning and deep learning methods including SVM, RF, LR, MLP, QDA, KNN, DT, 1D CNN, and C-CNN. In addition, the proposed models are carried out on EEG, EOG, EMG, and ECG signals, which are included in the DROZY dataset. Furthermore, two scenarios have been carried out for the classification, multiclass and binary-class scenarios. The proposed method achieves an accuracy of 96% with superior performance among the proposed efforts prior to fatigue detection.

However, the proposed approach has a drawback which is represented in the low performance of deep learning methods. Therefore, the performance can be enhanced in future work with some ideas. Using different feature selection and feature engineering algorithms will improve the performance by selecting some features with optimal importance. Another type of enhancement is to employ different optimization techniques to improve the performance of the deep learning approach. Furthermore, recurrent models can be considered and tested by the DROZY dataset.

Author Contributions: Conceptualization, methodology, software, validation, formal analysis, investigation, resources, writing—original draft preparation, A.S. and M.M.; writing—review and editing, visualization H.M. All authors have read and agreed to the published version of the manuscript.

Funding: Princess Nourah bint Abdulrahman University Researchers Supporting Project number (PNURSP2023R137): Princess Nourah bint Abdulrahman University, Riyadh, Saudi Arabia.

Acknowledgments: The authors would like to acknowledge the support of Prince Sultan University for paying the Article Processing Charges (APC) of this publication.

Conflicts of Interest: The authors declare no conflict of interest.

Abbreviations

SVM	Support Vector Machine
KNN	k-Nearest Neighbor
MLP	Multilayer Perceptron
RF	Random Forest
LR	Logistic Regression
DT	Decision Tree
QDA	Quadrature Data Analysis
CNN	Convolutional Neural Network
C-NN	Concatenated Convolutional Neural Network
MCC	Matthews Correlation Coefficient
ANN	Artificial Neural Network
FFT	Fast Fourier Transform
DWT	Discrete Wavelet Transform
DST	Discrete Sine Transform
DCT	Discrete Cosine Transform
EEG	Electroencephalogram
ECG	Electrocardiogram
EOG	Electrooculogram
EMG	Electromyogram
IoT	Internet of Things
FE	Fuzzy Entropy
SE	Sample Entropy
PSD	Power Spectral Density

References

1. Abbas, Q.; Alsheddy, A. Driver Fatigue Detection Systems Using Multi-Sensors, Smartphone, and Cloud-Based Computing Platforms: A Comparative Analysis. *Sensors* **2020**, *21*, 56. [CrossRef] [PubMed]
2. Ramzan, M.; Khan, H.U.; Awan, S.M.; Ismail, A.; Ilyas, M.; Mahmood, A. A Survey on State-of-the-Art Drowsiness Detection Techniques. *IEEE Access* **2019**, *7*, 61904–61919. [CrossRef]
3. Niloy, A.R.; Chowdhury, A.I.; Sharmin, N. A Brief Review on Different Driver's Drowsiness Detection Techniques. *Int. J. Image Graph. Signal Process.* **2020**, *10*, 41.

4. Choudhary, P.; Sharma, R.; Singh, G.; Das, S. A Survey Paper on Drowsiness Detection & Alarm System for Drivers. *Int. Res. J. Eng. Technol.* **2016**, *3*, 1433–1437.
5. Khan, M.Q.; Lee, S. A Comprehensive Survey of Driving Monitoring and Assistance Systems. *Sensors* **2019**, *19*, 2574. [CrossRef] [PubMed]
6. Chen, L.; Zhi, X.; Wang, H.; Wang, G.; Zhou, Z.; Yazdani, A.; Zheng, X. Driver Fatigue Detection via Differential Evolution Extreme Learning Machine Technique. *Electronics* **2020**, *9*, 1850. [CrossRef]
7. Fuletra, J.D.; Bosamiya, D. A Survey on Drivers Drowsiness Detection Techniques. *Int. J. Recent Innov. Trends Comput. Commun.* **2013**, *1*, 816–819.
8. Bergasa, L.M.; Nuevo, J.; Sotelo, M.A.; Barea, R.; Lopez, M.E. Real-Time System for Monitoring Driver Vigilance. *IEEE Trans. Intell. Transp. Syst.* **2006**, *7*, 63–77. [CrossRef]
9. Flores, M.J.; Armingol, J.M.; de la Escalera, A. Real-Time Warning System for Driver Drowsiness Detection Using Visual Information. *J. Intell. Robot. Syst.* **2010**, *59*, 103–125. [CrossRef]
10. Abtahi, S.; Hariri, B.; Shirmohammadi, S. Driver Drowsiness Monitoring Based on Yawning Detection. In Proceedings of the 2011 IEEE International Instrumentation and Measurement Technology Conference, Hangzhou, China, 10–12 May 2011; pp. 1–4.
11. Lenskiy, A.A.; Lee, J.-S. Driver's Eye Blinking Detection Using Novel Color and Texture Segmentation Algorithms. *Int. J. Control. Autom. Syst.* **2012**, *10*, 317–327. [CrossRef]
12. Jo, J.; Lee, S.J.; Kim, J.; Jung, H.G.; Park, K.R. Vision-Based Method for Detecting Driver Drowsiness and Distraction in Driver Monitoring System. *Opt. Eng.* **2011**, *50*, 127202. [CrossRef]
13. Malla, A.M.; Davidson, P.R.; Bones, P.J.; Green, R.; Jones, R.D. Automated Video-Based Measurement of Eye Closure for Detecting Behavioral Microsleep. In Proceedings of the 2010 annual international conference of the IEEE engineering in medicine and biology, Buenos Aires, Argentina, 31 August–4 September 2010; pp. 6741–6744.
14. Xiong, Y.; Gao, J.; Yang, Y.; Yu, X.; Huang, W. Classifying Driving Fatigue Based on Combined Entropy Measure Using EEG Signals. *Int. J. Control Autom.* **2016**, *9*, 329–338. [CrossRef]
15. Chai, R.; Naik, G.R.; Nguyen, T.N.; Ling, S.H.; Tran, Y.; Craig, A.; Nguyen, H.T. Driver Fatigue Classification with Independent Component by Entropy Rate Bound Minimization Analysis in an EEG-Based System. *IEEE J. Biomed. Health Inform.* **2016**, *21*, 715–724. [CrossRef]
16. Yin, J.; Hu, J.; Mu, Z. Developing and Evaluating a Mobile Driver Fatigue Detection Network Based on Electroencephalograph Signals. *Healthc. Technol. Lett.* **2017**, *4*, 34–38. [CrossRef] [PubMed]
17. Hu, J. Automated Detection of Driver Fatigue Based on AdaBoost Classifier with EEG Signals. *Front. Comput. Neurosci.* **2017**, *11*, 72. [CrossRef] [PubMed]
18. Min, J.; Wang, P.; Hu, J. Driver Fatigue Detection through Multiple Entropy Fusion Analysis in an EEG-Based System. *PLoS ONE* **2017**, *12*, e0188756. [CrossRef]
19. Ko, W.; Oh, K.; Jeon, E.; Suk, H.-I. Vignet: A Deep Convolutional Neural Network for Eeg-Based Driver Vigilance Estimation. In Proceedings of the 2020 8th International Winter Conference on Brain-Computer Interface (BCI), Gangwon, Republic of Korea, 26–28 February 2020; pp. 1–3.
20. Wang, Y.; Liu, X.; Zhang, Y.; Zhu, Z.; Liu, D.; Sun, J. Driving Fatigue Detection Based on EEG Signal. In Proceedings of the 2015 Fifth International Conference on Instrumentation and Measurement, Computer, Communication and Control (IMCCC), Qinhuangdao, China, 18–20 September 2015; pp. 715–718.
21. Zhendong, M.; Jinghai, Y. Mobile Healthcare System for Driver Based on Drowsy Detection Using EEG Signal Analysis. *Metall. Min. Ind.* **2015**, *7*, 266–273.
22. Nugraha, B.T.; Sarno, R.; Asfani, D.A.; Igasaki, T.; Munawar, M.N. Classification of driver fatigue state based on eeg using emotiv epoc+. *J. Theor. Appl. Inf. Technol.* **2016**, *86*.
23. Luo, H.; Qiu, T.; Liu, C.; Huang, P. Research on Fatigue Driving Detection Using Forehead EEG Based on Adaptive Multi-Scale Entropy. *Biomed. Signal Process. Control* **2019**, *51*, 50–58. [CrossRef]
24. Gao, Z.-K.; Li, Y.-L.; Yang, Y.-X.; Ma, C. A Recurrence Network-Based Convolutional Neural Network for Fatigue Driving Detection from EEG. *Chaos Interdiscip. J. Nonlinear Sci.* **2019**, *29*, 113126. [CrossRef]
25. Karuppusamy, N.S.; Kang, B.-Y. Multimodal System to Detect Driver Fatigue Using EEG, Gyroscope, and Image Processing. *IEEE Access* **2020**, *8*, 129645–129667. [CrossRef]
26. Aamir, M.; Rahman, Z.; Dayo, Z.A.; Abro, W.A.; Uddin, M.I.; Khan, I.; Imran, A.S.; Ali, Z.; Ishfaq, M.; Guan, Y. A Deep Learning Approach for Brain Tumor Classification Using MRI Images. *Comput. Electr. Eng.* **2022**, *101*, 108105. [CrossRef]
27. Aamir, M.; Pu, Y.-F.; Rahman, Z.; Tahir, M.; Naeem, H.; Dai, Q. A Framework for Automatic Building Detection from Low-Contrast Satellite Images. *Symmetry* **2018**, *11*, 3. [CrossRef]
28. Siam, A.I.; Soliman, N.F.; Algarni, A.D.; Abd El-Samie, F.E.; Sedik, A. Deploying Machine Learning Techniques for Human Emotion Detection. *Comput. Intell. Neurosci.* **2022**, *2022*, 8032673. [CrossRef]
29. El-Moneim, S.A.; Sedik, A.; Nassar, M.A.; El-Fishawy, A.S.; Sharshar, A.M.; Hassan, S.E.A.; Mahmoud, A.Z.; Dessouky, M.I.; El-Banby, G.M.; El-Samie, F.E.A.; et al. Text-Dependent and Text-Independent Speaker Recognition of Reverberant Speech Based on CNN. *Int. J. Speech Technol.* **2021**, *24*, 993–1006. [CrossRef]
30. Hammad, M.; Abd El-Latif, A.A.; Hussain, A.; Abd El-Samie, F.E.; Gupta, B.B.; Ugail, H.; Sedik, A. Deep Learning Models for Arrhythmia Detection in IoT Healthcare Applications. *Comput. Electr. Eng.* **2022**, *100*, 108011. [CrossRef]

31. Ibrahim, F.E.; Emara, H.M.; El-Shafai, W.; Elwekeil, M.; Rihan, M.; Eldokany, I.M.; Taha, T.E.; El-Fishawy, A.S.; El-Rabaie, E.M.; Abdellatef, E. Deep Learning-based Seizure Detection and Prediction from EEG Signals. *Int. J. Numer. Method. Biomed. Eng.* **2022**, *38*, e3573. [CrossRef]
32. Shoaib, M.R.; Emara, H.M.; Elwekeil, M.; El-Shafai, W.; Taha, T.E.; El-Fishawy, A.S.; El-Rabaie, E.-S.M.; El-Samie, F.E.A. Hybrid Classification Structures for Automatic COVID-19 Detection. *J. Ambient Intell. Humaniz. Comput.* **2022**, *13*, 4477–4492. [CrossRef]
33. Daoui, A.; Yamni, M.; Karmouni, H.; Sayyouri, M.; Qjidaa, H.; Motahhir, S.; Jamil, O.; El-Shafai, W.; Algarni, A.D.; Soliman, N.F. Efficient Biomedical Signal Security Algorithm for Smart Internet of Medical Things (IoMTs) Applications. *Electronics* **2022**, *11*, 3867. [CrossRef]
34. Li, L.; Jamieson, K.; DeSalvo, G.; Rostamizadeh, A.; Talwalkar, A. Hyperband: A Novel Bandit-Based Approach to Hyperparameter Optimization. *J. Mach. Learn. Res.* **2017**, *18*, 6765–6816.
35. Crammer, K.; Singer, Y. On the Algorithmic Implementation of Multiclass Kernel-Based Vector Machines. *J. Mach. Learn. Res.* **2001**, *2*, 265–292.
36. Massoz, Q.; Langohr, T.; François, C.; Verly, J.G. The ULg Multimodality Drowsiness Database (Called DROZY) and Examples of Use. In Proceedings of the 2016 IEEE Winter Conference on Applications of Computer Vision (WACV), Lake Placid, NY, USA, 7–10 March 2016; pp. 1–7.
37. Chicco, D.; Jurman, G. The Advantages of the Matthews Correlation Coefficient (MCC) over F1 Score and Accuracy in Binary Classification Evaluation. *BMC Genom.* **2020**, *21*, 6. [CrossRef] [PubMed]
38. Karpiński, R. Knee Joint Osteoarthritis Diagnosis Based on Selected Acoustic Signal Discriminants Using Machine Learning. *Appl. Comput. Sci.* **2022**, *18*, 71–85. [CrossRef]
39. Karpiński, R.; Krakowski, P.; Jonak, J.; Machrowska, A.; Maciejewski, M.; Nogalski, A. Diagnostics of Articular Cartilage Damage Based on Generated Acoustic Signals Using ANN—Part II: Patellofemoral Joint. *Sensors* **2022**, *22*, 3765. [CrossRef] [PubMed]
40. Correa, A.G.; Orosco, L.; Laciar, E. Automatic Detection of Drowsiness in EEG Records Based on Multimodal Analysis. *Med. Eng. Phys.* **2014**, *36*, 244–249. [CrossRef]
41. Ko, L.-W.; Lai, W.-K.; Liang, W.-G.; Chuang, C.-H.; Lu, S.-W.; Lu, Y.-C.; Hsiung, T.-Y.; Wu, H.-H.; Lin, C.-T. Single Channel Wireless EEG Device for Real-Time Fatigue Level Detection. In Proceedings of the 2015 International Joint Conference on Neural Networks (IJCNN), Killarney, Ireland, 12–17 July 2015; pp. 1–5.
42. Liu, Y.; Lan, Z.; Cui, J.; Sourina, O.; Müller-Wittig, W. Inter-Subject Transfer Learning for EEG-Based Mental Fatigue Recognition. *Adv. Eng. Inform.* **2020**, *46*, 101157. [CrossRef]